

# A coherent modified Redfield theory for excitation energy transfer in molecular aggregates



Yu-Hsien Hwang-Fu, Wei Chen, Yuan-Chung Cheng\*

Department of Chemistry, Center for Quantum Science and Engineering, National Taiwan University, Taipei City 106, Taiwan

## ARTICLE INFO

### Article history:

Received 19 September 2014

In final form 30 November 2014

Available online 11 December 2014

### Keywords:

Coherent modified Redfield theory

Excitation energy transfer

Light harvesting

Quantum master equation

## ABSTRACT

Excitation energy transfer (EET) is crucial in photosynthetic light harvesting, and quantum coherence has been recently proven to be a ubiquitous phenomenon in photosynthetic EET. In this work, we derive a coherent modified Redfield theory (CMRT) that generalizes the modified Redfield theory to treat coherence dynamics. We apply the CMRT method to simulate the EET in a dimer system and compare the results with those obtained from numerically exact path integral calculations. The comparison shows that CMRT provides excellent computational efficiency and accuracy within a large EET parameter space. Furthermore, we simulate the EET dynamics in the FMO complex at 77 K using CMRT. The results show pronounced non-Markovian effects and long-lasting coherences in the ultrafast EET, in excellent agreement with calculations using the hierarchy equation of motion approach. In summary, we have successfully developed a simple yet powerful framework for coherent EET dynamics in photosynthetic systems and organic materials.

© 2014 Elsevier B.V. All rights reserved.

## 1. Introduction

Excitation energy transfer (EET) is a crucial process in photosynthetic light harvesting. The near unity efficiency of photosynthetic EET from the antenna to the reaction center ensures the success of energy collections in light reactions, and thus enables the subsequent sugar-production reactions that support life forms on earth [1,2]. In addition to natural photosynthesis, EET also occurs in synthetic photosensitive molecules and conjugate polymers, which are potential materials for energy applications. Because of the importance and ubiquity of EET, its mechanism and accurate dynamical simulations have become an intriguing subject to scientists for decades [3,4]. Recent ultrafast time-resolved spectroscopic experiments revealing the existence of long-lived quantum coherence in photosynthetic complexes and conjugated polymer systems have been a major breakthrough in this field [5–8]. Although the significance of coherent EET in photosynthetic efficiency remains controversial, these experiments clearly demonstrate that conventional theories for EET can not adequately describe ultrafast (<picosecond time scale) transfer dynamics that are commonly observed in photosynthesis and bulk organic optoelectronic materials.

The major difficulty in describing coherent EET in molecular aggregate systems is how to appropriately treat the electronic coupling between the pigments and the exciton–phonon coupling between the excitations and their surrounding environments in a balanced way. A number of new frameworks employing various techniques, such as polaron transformation [9–12], quantum–classical hybrid methods [13–15], and non-perturbative approaches [16–25], have been suggested recently. In this study we turn to the modified Redfield theory [26,27], which has been applied to describe population dynamics and spectra of many photosynthetic systems. Unlike the conventional Redfield theory, the modified Redfield theory treats only the off-diagonal part of the exciton–phonon coupling matrix as the perturbation. As a result, it correctly and smoothly interpolates between the Förster and the Redfield theories at their respective limits [27,28]. Thus, the modified Redfield theory has been a popular tool in studies of light harvesting EET [29,28,3,30]. Recently, Novoderezhkin and van Grondelle have comprehensively evaluated the validity of the modified Redfield theory by benchmarking it against other theoretical methods [28,4] and by applying it to fit experimental data [31,29,32]. They conclude that a combination of modified Redfield approach and generalized Förster theory [33] yields excellent simulations of EET dynamics in photosynthetic systems [32]. Despite its popularity in photosynthetic EET, the modified Redfield theory cannot be applied to model coherent EET since coherence dynamics are neglected fully. Therefore, recently revealed coherent EET

\* Corresponding author.

E-mail address: [yuanchung@ntu.edu.tw](mailto:yuanchung@ntu.edu.tw) (Y.-C. Cheng).

phenomena in natural photosynthetic systems can not be described by the conventional modified Redfield theory.

Previously, Golosov and Reichman have proposed a pure dephasing reference system (PDRS) master equation that in essence is the full quantum master equation in the same basis of the modified Redfield theory [34,35]. The PDRS approach was shown to provide excellent results in a broad parameter space of the electron transfer problem, however, the complicated equation of motion made its application to large multichromophoric photosynthetic systems a formidable task.

In this work, we aim to derive a simple yet powerful quantum master equation based on the framework of the modified Redfield approach. This coherent modified Redfield theory (CMRT) allows the description of coherent EET dynamics as well as time-resolved spectroscopic signals that depend on the coherences. Additionally, to capture non-equilibrium bath relaxation effects, we do not apply the Markovian approximation, and thus the dissipation tensor is kept time-dependent. We also consider a generalized form of line-shape functions that enables the treatment of correlated-bath effects. Furthermore, we present the applications of this new framework, with comparisons to numerically exact methods. We explore the properties of CMRT in a simple two-site system and compare the results with those obtained from the quasi-adiabatic propagator path integral (QUAPI) approach. Finally, we compare our simulation of EET dynamics in the Fenna–Matthews–Olson complex with the exact results from the reduced hierarchy equation approach to show the effectiveness of the CMRT approach for coherent EET dynamics in photosynthetic systems.

## 2. Theoretical method

In order to develop a general theory for EET we adopted the modified Redfield theory [26] and extended it to treat coherent evolution of excitonic systems. In this section we describe the derivation of the CMRT equation of motion.

### 2.1. Model Hamiltonian

In this study, we employ the Frenkel exciton Hamiltonian to describe photoexcitations of a molecular aggregate with  $N$  sites. Written in the electronic eigenbasis (the so called exciton basis), the Hamiltonian reads ( $\hbar = 1$ ):

$$H = H_e + H_{ph} + H_{e-ph},$$

$$H_e = \sum_{\alpha=1}^N \varepsilon_{\alpha} |\alpha\rangle\langle\alpha|, \quad (1)$$

$$H_{ph} = \sum_i \omega_i b_i^{\dagger} b_i, \quad (2)$$

$$\begin{aligned} H_{e-ph} &= \sum_{\alpha,\beta} |\alpha\rangle\langle\beta| \cdot \sum_{n=1}^N \sum_i c_n^{\alpha} c_n^{\beta*} g_{ni} \omega_i (b_i + b_i^{\dagger}) \\ &\equiv \sum_{\alpha,\beta} |\alpha\rangle\langle\beta| \cdot (H_{e-ph})_{\alpha\beta}, \end{aligned} \quad (3)$$

where  $|\alpha\rangle$  denotes the  $\alpha$ th exciton state, which is a delocalized linear combination of site excitations,  $|\alpha\rangle = \sum_n c_n^{\alpha} |n\rangle$ . In addition,  $\varepsilon_{\alpha}$  denotes the excitation energy of  $|\alpha\rangle$ ,  $b_i^{\dagger}$  ( $b_i$ ) is the creation (annihilation) operator of the  $i$ th phonon mode,  $\omega_i$  is the frequency of the phonon mode, and  $g_{ni}$  is the exciton–phonon coupling constant between the localized electronic excitation on site  $n$  and the  $i$ th phonon mode. Note that we do not limit ourself to localized phonon modes, so general correlated baths are described in this model. The exciton–phonon coupling constant is related to the displacement of

the phonon coordinate in the excited state, which also defines the site reorganization energy  $\lambda_n = \sum_i \sum_n g_{ni}^2 \omega_i$ . Finally, basis transformation from the site basis to the exciton basis yields the  $\sum_n c_n^{\alpha} c_n^{\beta}$  factor, which can be considered as the overlap between exciton wavefunctions  $|\alpha\rangle$  and  $|\beta\rangle$ .

The main idea behind the modified Redfield theory [26] is to partition the Hamiltonian into a zeroth-order Hamiltonian including the diagonal fluctuations in the exciton basis:

$$H_0 = H_e + H_{ph} + \sum_{\alpha=1}^N |\alpha\rangle\langle\alpha| \cdot (H_{e-ph})_{\alpha\alpha}$$

and a perturbation part:

$$V = \sum_{\alpha \neq \beta} |\alpha\rangle\langle\beta| \cdot (H_{e-ph})_{\alpha\beta}.$$

Specifically, the diagonal part of  $H_{e-ph}$  (Eq. (3)) is included in the zeroth-order Hamiltonian while the perturbation part includes only the off-diagonal part of  $H_{e-ph}$ . By treating the diagonal part of  $H_{e-ph}$  nonperturbatively, bath reorganizations and pure dephasing are treated exactly in this formalism. Moreover, multi-phonon effects are included [27,28]. Base on the same partitioning of the zeroth-order Hamiltonian, we derive a coherent modified Redfield theory for coherent EET dynamics.

### 2.2. Quantum master equation

The modified Redfield theory was derived with a diagonal projection operator, which omits the coherence part of the density matrix and only considers the population transfer between exciton states [26,27]. Given that recent experimental and theoretical studies have shown coherent EET dynamics in natural photosynthetic complexes and organic conjugated polymers, it is highly desirable to extend the modified Redfield theory to treat coherent dynamics. To this end, we start from a general time-local quantum master equation that is derived using a second-order cumulant expansion technique with respect to a perturbation  $V$  [36,37]. The quantum master equation written in the interaction picture of  $H_0$  is

$$\dot{\sigma}_I(t) = - \int_0^t d\tau \text{Tr}_B \{ [V_I(t), [V_I(\tau), \sigma_I(\tau) \otimes \rho_b^{eq}]] \}, \quad (4)$$

where  $V_I(t)$  is defined in the interaction picture of  $H_0$ , i.e.  $V_I(t) = e^{iH_0 t} V(t) e^{-iH_0 t}$ . Note that to derive Eq. (4), we have assumed a product-state initial condition,  $\rho(0) = \sigma(0) \rho_b^{eq}$ , where  $\rho_b^{eq} = e^{-\beta H_{ph}} / Z$  is the equilibrium density matrix of the bath. This assumption is justified with photoinduced EET processes. Additionally, we also neglect the first-order average of the perturbation, i.e.  $\langle V \rangle$  in the perturbation. This greatly simplifies the equation of motion, however, it can not be easily justified. In this work we perform numerical simulations to demonstrate that neglecting the first-order term does not contribute to significant error in a broad parameter regime.

In the Schrödinger picture, the reduced density matrix is calculated by

$$\sigma(t) = \text{Tr}_B \{ U_0(t) \sigma_I(t) \rho_b^{eq} U_0^{\dagger}(t) \}.$$

Note that  $U_0(t)$  can not be simply separated into a system part and a bath part. Because the diagonal exciton–phonon coupling term contains both system and bath operators, the partial trace has to be taken *after* solving  $U_0(t) \sigma_I(t) U_0^{\dagger}(t)$ . Formally, the equation of motion for the reduced density matrix is

$$\begin{aligned} \dot{\sigma}(t) &= -i \text{Tr}_B \{ [H_0, \sigma(t) \otimes \rho_b^{eq}] \} \\ &\quad - \int_0^t \text{Tr}_B \{ [V, [V(-\tau), \sigma(t) \otimes \rho_b^{eq}]] \} d\tau \\ &= \dot{\sigma}^{(coh)}(t) + \dot{\sigma}^{(diss)}(t). \end{aligned} \quad (5)$$

In Eq. (5), we separate the time evolution of the reduced density matrix into a coherent part driven by  $H_0$  and a dissipative part containing  $V$ . In the following we will discuss these two parts separately.

### 2.2.1. Coherent dynamics

The coherent part in Eq. (5) describes the excitonic coherent evolution and the pure dephasing of the density matrix in the exciton basis. To describe the coherent evolution, we consider the time evolution of  $\sigma(t)$  driven by the zeroth order Hamiltonian  $H_0$ :

$$\sigma^{(coh)}(t) = \text{Tr}_B \{ U_0(t) \sigma(0) \rho_b^{eq} U_0^\dagger(t) \},$$

which can be evaluated exactly to yield the density matrix elements:

$$\sigma_{\alpha\beta}^{(coh)}(t) = e^{-i(\varepsilon_\alpha - \varepsilon_\beta)t} \cdot \text{Tr}_B \left\{ e^{-i(H_{ph} + H_{e-ph}^{zz})t} \rho_b^{eq} e^{i(H_{ph} + H_{e-ph}^{\beta\beta})t} \right\} \cdot \sigma_{\alpha\beta}(0). \quad (6)$$

In Eq. (6), the first term describes the coherent evolution driven by the exciton Hamiltonian, and the second term yields the pure dephasing of the coherences. The pure dephasing is caused by exciton energy fluctuations induced by the diagonal exciton–phonon couplings, and this contribution is unique to the CMRT theory. Note that the  $\sigma_{\alpha\beta}^{(coh)}(t)$  term does not contribute to the population dynamics when  $\alpha = \beta$  (population terms). After evaluating the thermal average with displacement operators and take the derivative in time, we obtain

$$\dot{\sigma}_{\alpha\beta}(t) = \left[ -i(\varepsilon_\alpha - \varepsilon_\beta)t - R_{\alpha\beta}^{pd}(t) \right] \sigma_{\alpha\beta}(t), \quad (7)$$

where the pure-dephasing rate  $R_{\alpha\beta}^{pd}(t)$  is defined as

$$R_{\alpha\beta}^{pd}(t) = \text{Re} [\dot{g}_{\alpha\alpha\alpha\alpha}(t) + \dot{g}_{\beta\beta\beta\beta}(t) - 2\dot{g}_{\alpha\alpha\beta\beta}(t)] + i \text{Im} [\dot{g}_{\alpha\alpha\alpha\alpha}(t) - \dot{g}_{\beta\beta\beta\beta}(t)], \quad (8)$$

In Eq. (8), we have used the lineshape function  $g(t)$  defined as

$$g_{\alpha\beta\gamma\delta}(t) = \int_0^t dt_1 \int_0^{t_1} dt_2 \langle H_{\alpha\beta}^{el-ph}(t_1) H_{\gamma\delta}^{el-ph}(t_2) \rangle. \quad (9)$$

The time-correlation function in the integral depends on the exciton–phonon couplings. In condensed phased systems, the number of phonon modes coupled to the excitons is so large that we should use spectral density functions to describe such interactions. Here we define general spectral density functions,  $J_{nm}(\omega)$ , as coupling-weighted density of states:

$$J_{nm}(\omega) = \sum_i g_{ni} g_{mi} \omega_i^2 \delta(\omega - \omega_i). \quad (10)$$

Note that the spectral density is site-dependent and the definition generalizes the spectral density function to treat correlated-bath conditions. Diagonal  $J_{nn}(\omega)$  describes spectral density of site energy fluctuations on site  $n$ , while  $J_{nm}(\omega)$  describes cross correlations between site energy fluctuations on  $n$  and  $m$ . The lineshape function at exciton basis considering general bath spectral density functions  $J_{nm}(\omega)$  can be evaluated from Eq. (10) to obtain

$$g_{\alpha\beta\gamma\delta}(t) = \sum_{n,m} c_n^\alpha c_n^{\beta*} c_m^\gamma c_m^{\delta*} \int_0^\infty d\omega \frac{J_{nm}(\omega)}{\omega^2} \left\{ \coth\left(\frac{\omega}{2k_B T}\right) [1 - \cos(\omega t)] + i[\sin(\omega t) - \omega t] \right\} + \sum_{n,m} c_n^\alpha c_n^{\beta*} c_m^\gamma c_m^{\delta*} \cdot g_{nm}(t). \quad (11)$$

Therefore, after the spectral densities  $J_{nm}(\omega)$  are specified, the lineshape functions can then be evaluated to calculate EET dynamics using the CMRT approach. We emphasize that this form of lineshape functions treats correlated-bath effects therefore the formalism presented in this work is not limited to independent-bath models.

### 2.2.2. Dissipation

The second term in Eq. (5) describes the dissipative dynamics:

$$\dot{\sigma}^{(diss)}(t) = - \int_0^t d\tau \text{Tr}_B \{ [V, [V(-\tau), \sigma(t) \otimes \rho_b^{eq}]] \}, \quad (12)$$

which can be evaluated to yield

$$\dot{\sigma}_{\alpha\beta}^{(diss)}(t) = \sum_{\gamma\delta} \left( \Gamma_{\delta\beta,\alpha\gamma} + \Gamma_{\gamma\alpha,\beta\delta}^* - \delta_{\beta\delta} \sum_f \Gamma_{\alpha f, f\gamma} - \delta_{\alpha\gamma} \sum_f \Gamma_{\beta f, f\delta}^* \right) \sigma_{\gamma\delta}(t), \quad (13)$$

where

$$\Gamma_{\alpha\beta,\gamma\delta} = \int_0^t d\tau \langle V_{\alpha\beta} V_{\gamma\delta}(-\tau) \rangle. \quad (14)$$

In Eq. (14),  $V_{\alpha\beta}(-\tau) = \langle \alpha | V(-\tau) | \beta \rangle$ . In general, from Eq. (12) the full Redfield tensor can be calculated in the modified Redfield representation. However, to reach a simple equation of motion, we employ the secular approximation, and consider only population transfer and dephasing of coherences. Here, non-secular terms could affect the dynamics, but a detailed analysis of these issues would be out of the scope of this paper. Given the success of modified Redfield theory in describing photosynthetic EET, we believe the current secular approach provides an effective and useful approximation. Under the approximation, we require  $\alpha = \beta$ ,  $\gamma = \delta$ , or  $\alpha \neq \beta$ ,  $\gamma = \alpha$ ,  $\delta = \beta$ , which lead to the population transfer and the dephasing processes, respectively.

*Population Transfer* ( $\alpha = \beta$ ,  $\gamma = \delta$ ):

The population transfer term in the CMRT is the same as that in the modified Redfield theory. Therefore,

$$\dot{\sigma}_{\alpha\alpha}^{(diss)}(t) = \sum_{\gamma} (R_{\alpha\gamma} \sigma_{\gamma\gamma}(t) - R_{\gamma\alpha} \sigma_{\alpha\alpha}(t)). \quad (15)$$

The transfer rate from  $|\beta\rangle$  state to  $|\alpha\rangle$  state is given by

$$R_{\alpha\beta}(t) = 2 \cdot \text{Re} \int_0^t d\tau \langle V_{\beta\alpha} V_{\alpha\beta}(-\tau) \rangle. \quad (16)$$

Eq. (16) can be evaluated to yield:

$$R_{\alpha\beta}(t) = 2 \cdot \text{Re} \int_0^t d\tau F_{\beta}^*(\tau) A_{\alpha}(\tau) X_{\alpha\beta}(\tau), \quad (17)$$

where

$$A_{\alpha}(t) = e^{-i\varepsilon_{\alpha} t - g_{\alpha\alpha\alpha\alpha}(t)},$$

$$F_{\alpha}(t) = e^{-i(\varepsilon_{\alpha} - 2g_{\alpha\alpha\alpha\alpha})t - g_{\alpha\alpha\alpha\alpha}^*(t)}$$

and the perturbation induced dynamical term can be evaluated to yield

$$X_{\alpha\beta}(t) = e^{2(g_{\alpha\alpha\beta\beta}(t) + i\lambda_{\alpha\beta\beta\beta} t)} \times [\dot{g}_{\beta\alpha\alpha\alpha}(t) - (\dot{g}_{\beta\alpha\alpha\alpha}(t) - \dot{g}_{\beta\alpha,\beta\beta}(t) - 2i\lambda_{\beta\alpha\beta\beta}) \times (\dot{g}_{\alpha\beta\alpha\alpha}(t) - \dot{g}_{\alpha\beta\beta\beta}(t) - 2i\lambda_{\alpha\beta\beta\beta})],$$

where  $g_{\alpha\beta\gamma\delta}(t)$  is the lineshape function defined in Eq. (11), and  $A(t)$  and  $F(t)$  are related to the absorption and emission lineshape, respectively [4,28].

*Dephasing* ( $\alpha \neq \beta$ ,  $\gamma = \alpha$ ,  $\delta = \beta$ ):

The off-diagonal exciton–phonon couplings in the exciton basis not only give rise to population transfer dynamics, they also induce dephasing of the coherences. The dephasing term can be evaluated to yield

$$\dot{\sigma}_{\alpha\beta}^{(diss)}(t) = - \left( \frac{1}{2} \sum_f (R_{f\alpha} + R_{f\beta}) + i \cdot \text{Im} \sum_f (\Gamma_{\alpha f, f\alpha} + \Gamma_{\beta f, f\beta}^*) \right) \sigma_{\alpha\beta}(t). \quad (18)$$

The dephasing is related to the population transfer and the imaginary part of the exciton–phonon coupling time-correlation

functions. According to several numerical calculations, the imaginary terms have only minor effects on the EET dynamics. Thus, for the simplicity of the formalism, we decided to drop the imaginary part in Eq. (18) in all the calculations presented in this work. Moreover, according to Eq. (18), the rate of the population-transfer induced dephasing is exactly half of that of the population transfer. Hence, this model follows the standard  $1/T_2 = 1/2T_1 + 1/T_2^*$  relationship. Finally, we remark that this equation is in the secular form and can be rewritten in a generalized Lindblad form [38], therefore the positivity violation problem should be avoided.

### 2.3. Coherent modified Redfield theory

Collecting the results in the previous section, we obtained a quantum master equation from second-order cumulant expansion and secular approximation:

$$\dot{\sigma}_{\alpha\beta}(t) = -i(\varepsilon_\alpha - \varepsilon_\beta)\sigma_{\alpha\beta}(t) + \sum_f [R_{\alpha f}(t)\sigma_{ff}(t) - R_{f\alpha}(t)\sigma_{\alpha\alpha}(t)] \cdot \delta_{\alpha\beta} - \left[ R_{\alpha\beta}^{pd}(t) + \frac{1}{2} \sum_f (R_{f\alpha}(t) + R_{f\beta}(t)) \right] \sigma_{\alpha\beta}(t). \quad (19)$$

Eq. (19) is the main result of this work, and it is a direct extension of the original modified Redfield theory to include coherence dynamics. We therefore call it the coherent modified Redfield

theory (CMRT). The CMRT has very clear physical interpretation for each term. The first term in Eq. (19) describes the coherent dynamics driven by the pure excitonic Hamiltonian, the second term is population transfer due to off-diagonal exciton–phonon couplings in the exciton basis, and the last term represents the dephasing of coherences, which includes both the pure dephasing (determined by rate  $R_{\alpha\beta}^{pd}$ ) and the population transfer induced dephasing (determined by  $R_{f\alpha}$ ). In addition, the CMRT equation of motion is non-Markovian. To go beyond the Markovian limit adopted in the original modified Redfield theory, we preserve the time dependence of the Redfield tensor. This master equation has the same form as the traditional Redfield equation, and is easy to propagate and applicable to large multichromophoric systems. Furthermore, the dephasing terms in CMRT in Eq. (19) clearly lead to the same expression for absorption spectrum with lifetime broadening effects proposed by Novoderenskin and van Grondelle [4]. The inclusion of coherent dynamics in CMRT makes it possible to directly include the influence of external fields in the simulation, thus significantly expands the applicability of the theory to problems to which the original modified Redfield theory is not applicable, such as time-resolved spectroscopy and control problems.

Note that the secular approximation not only greatly simplifies the equation, it also enhances the stability and applicability of the CMRT, as often found in similar second order approaches [39–41]. However, the secular approximation also neglects coherence

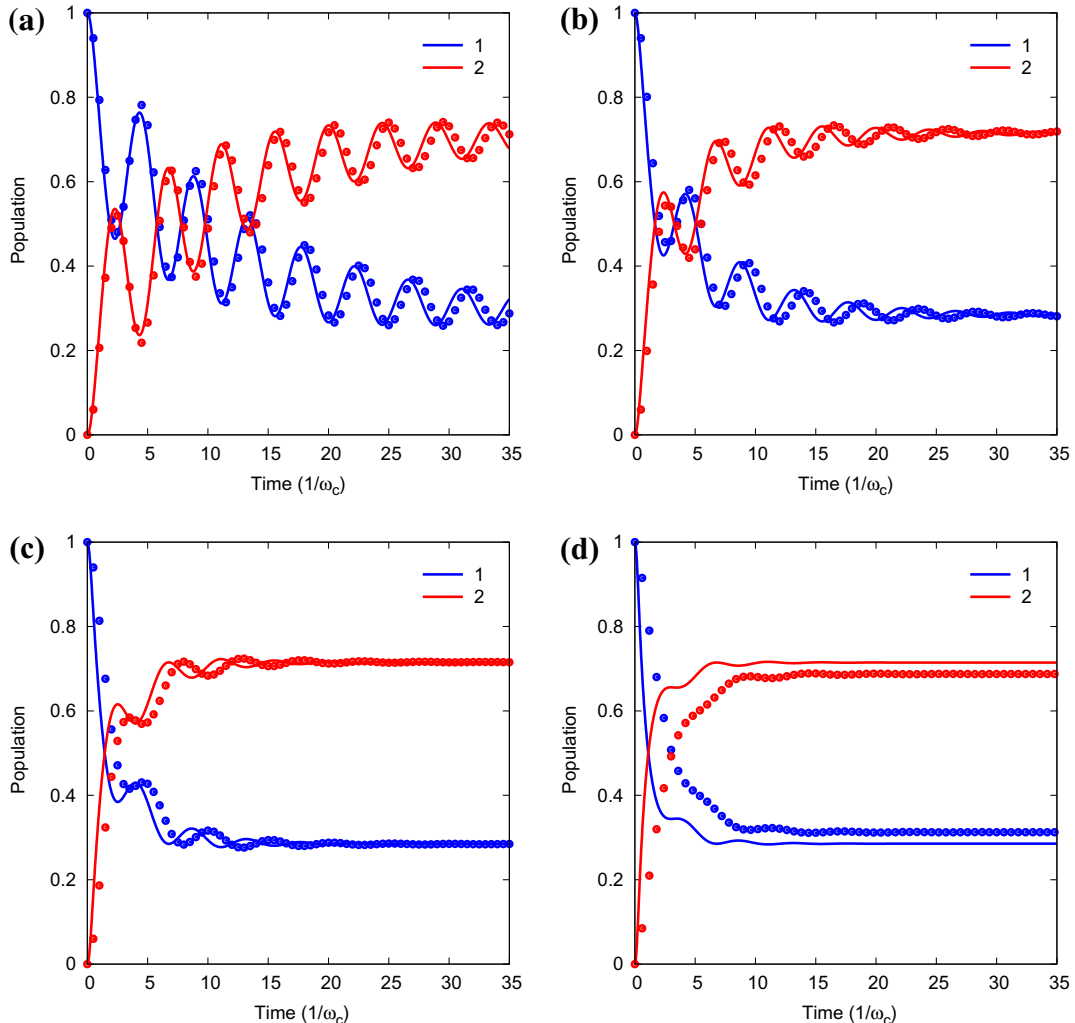


**Fig. 1.** Comparisons of population dynamics between CMRT (solid lines) and QUAPI (dots) in the coherent regime with different system-bath coupling strengths. (a)  $\gamma = 0.2$ . (b)  $\gamma = 0.5$ . (c)  $\gamma = 1$  (d)  $\gamma = 2$ . Other parameters are:  $\Delta/\omega_c = 0.5$ ,  $J/\omega_c = 0.5$ , and  $\beta\omega_c = 1$ .

dynamics such as population to coherence transfer, which could be important in some systems [42,4]. Nevertheless, a full CMRT approach can be achieved by removing the secular approximation, however, as the approach is still perturbative it does not guarantee to improve the results in all parameter regimes. Since our goal is to develop an approximated theory that can be applied to study EET in a complete photosynthetic supercomplex with hundreds of chlorophylls, we believe the secular CMRT strikes the balance between numerical efficiency and accuracy. The validity of the secular approximation and the possible effects caused by the coherence transfer are interesting issues worth thorough investigations, but these are beyond the scope of this work.

The CMRT approach adopts the same basis of the modified Redfield theory, therefore we expect it to have similar range of applicability as the original modified Redfield theory. The applicability of the modified Redfield theory to determine population transfer rates between exciton states beyond the traditional Redfield theory and Förster theory was already examined by Yang and Fleming, and they concluded that the success of the modified Redfield theory is mostly due to its incorporation of multi-phonon processes [27]. Moreover, recent studies have demonstrated that modified Redfield theory yields unphysical population transfer rates at small electronic coupling and small energy gap, because dynamical localization is not treated properly [28,4]. The aim of this work is to extend the modified Redfield theory to include coherent dynamics, therefore a rigorous validation of its

assumptions is outside of the scope of this paper and is currently a work in progress.

### 3. Dynamics of a dimer system

To demonstrate the validity of the CMRT approach, we apply it to calculate EET dynamics for a model dimer donor–acceptor system in a broad parameter regime. The dimer is described by the electronic Hamiltonian in the site-representation using site excitations  $|1\rangle$  and  $|2\rangle$  as the basis:

$$H_S = \begin{bmatrix} \Delta & J_0 \\ J_0 & -\Delta \end{bmatrix},$$

where sites 1 and 2 are the donor and acceptor, respectively. In addition, we assume site-independent baths and site-diagonal exciton-phonon coupling represented by the super-Ohmic Debye spectral density  $J_{11}(\omega) = J_{22}(\omega) = \gamma\omega^3 e^{-\omega/\omega_c} / \pi\omega_c^2$ , where  $\gamma$  is the exciton-phonon coupling strength and  $\omega_c$  is the cut-off frequency of the bath; and herein we do not consider cross-correlations, i.e.  $J_{12}(\omega) = 0$ .

In Fig. 1, we show the population dynamics calculated from CMRT for a dimer system with  $\Delta/\omega_c = 0.5$ ,  $J/\omega_c = 0.5$ , and  $\beta\omega_c = 1$  at different exciton–phonon coupling strengths, together with the results calculated from the quasiadiabatic propagator path integral method (QUAPI). QUAPI is a numerically exact method based on the path integral approach to quantum dynamics,

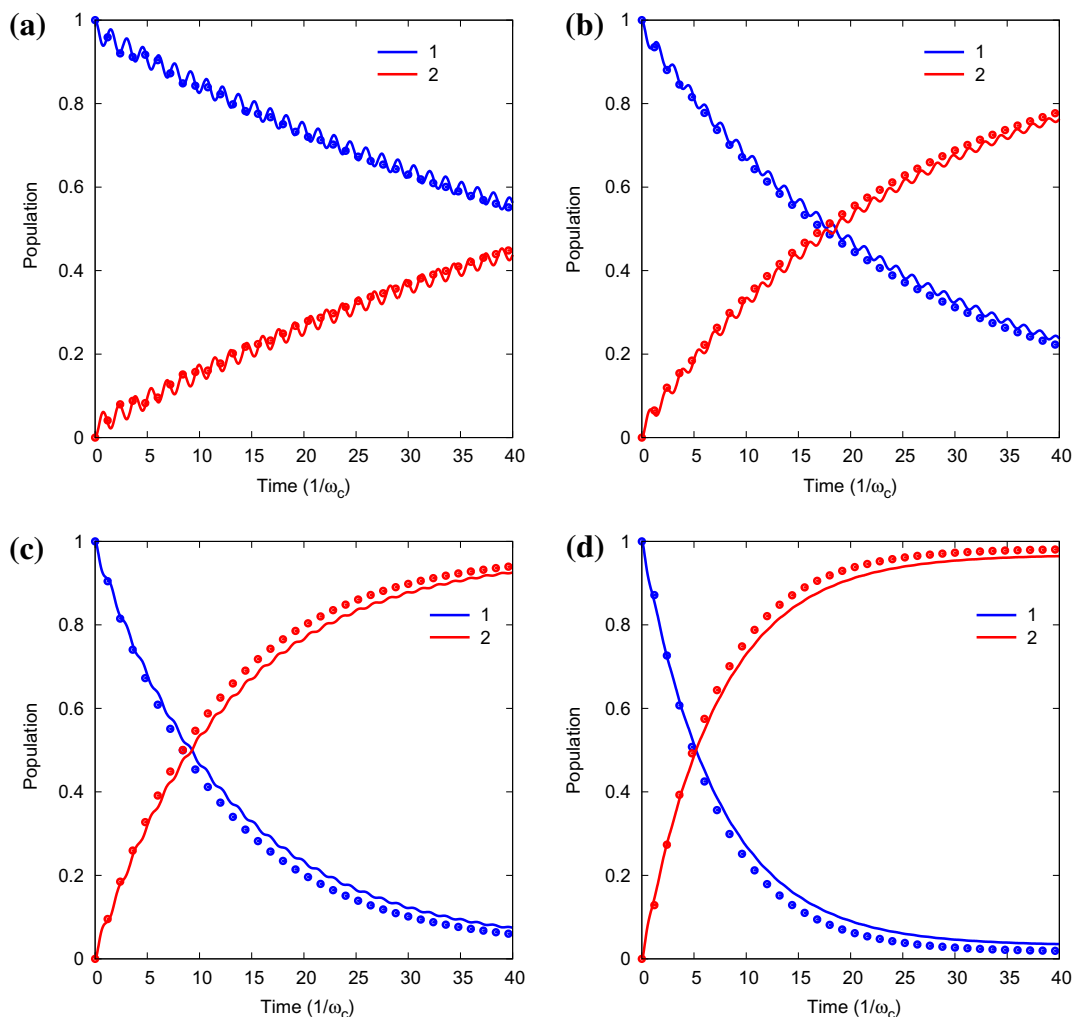


**Fig. 2.** Comparisons of population dynamics between CMRT (solid lines) and QUAPI (dots) in the incoherent regime. (a)  $\gamma = 0.2$ . (b)  $\gamma = 0.5$ . (c)  $\gamma = 1$  (d)  $\gamma = 2$ . Other parameters are:  $\Delta/\omega_c = 2$ ,  $J/\omega_c = 0.5$ , and  $\beta\omega_c = 1$ .



and the QUAPI results used in this work are taken from Ref. [43]. At weak exciton–phonon couplings (coherent regime), the CMRT correctly describes coherent dynamics to yield excellent results, with only a minor frequency error that can be attributed to that the pure excitonic exciton basis adopted in the CMRT formalism overestimates the energy gap between the two eigenstates. At stronger exciton–phonon couplings, however, CMRT begins to deviate from the exact result by overestimating the population transfer rates. This occurs when the exciton–bath coupling is greater than the bias between the two sites, again can be attributed to the problem of the exciton basis. There, dynamical localization and polaron formation, which are neglected in CMRT, could significantly influence the EET dynamics [44–46,23]. The neglect of dynamical localization in CMRT overestimates the delocalization of the eigenstates, and in such large exciton–phonon coupling limit, the generalized Förster theory is actually more appropriate [28,4]. Nevertheless, Fig. 1 shows that CMRT correctly captures coherent dynamics and performs quite well at weak to intermediate exciton–phonon couplings. In addition, the coherent to incoherent dynamical transition induced by increase of exciton–phonon coupling is correctly described. Thus, we have successfully extended the modified Redfield theory to treat coherent EET dynamics.

Moreover, in Fig. 2 we show EET dynamics for a dimer in the incoherent regime ( $\Delta/\omega_c = 2$ ,  $J/\omega_c = 0.5$ , and  $\beta\omega_c = 1$ ). Clearly, CMRT yields excellent results at all exciton–phonon coupling strengths for this system with large site-energy gap ( $\Delta/J \gg 1$ ). In this case, the excitons are quite localized, therefore the problem of overly delocalized zeroth-order states does not exist. Generally speaking, we conclude that the CMRT method yields excellent results at weak exciton–phonon couplings and large site-energy gaps.

#### 4. FMO dynamics

To further examine the effectiveness of using CMRT to simulate photosynthetic EET, we apply it to calculate EET dynamics of a model for the monomeric subunit of the Fenna–Matthews–Olson (FMO) complex from green sulfur bacteria, and compare the results with numerically exact simulation carried out by Ishizaki and Fleming. The FMO complex is a photosynthetic complex with seven bacteriachlorophyll chromophores (Fig. 3(a)). It functions as an “energy wire” to direct excitation energy from the light-harvesting antenna to the reaction center [47]. Due to its small size and early availability of crystal structure, the FMO complex has been studied extensively and is an important model system in photosynthetic

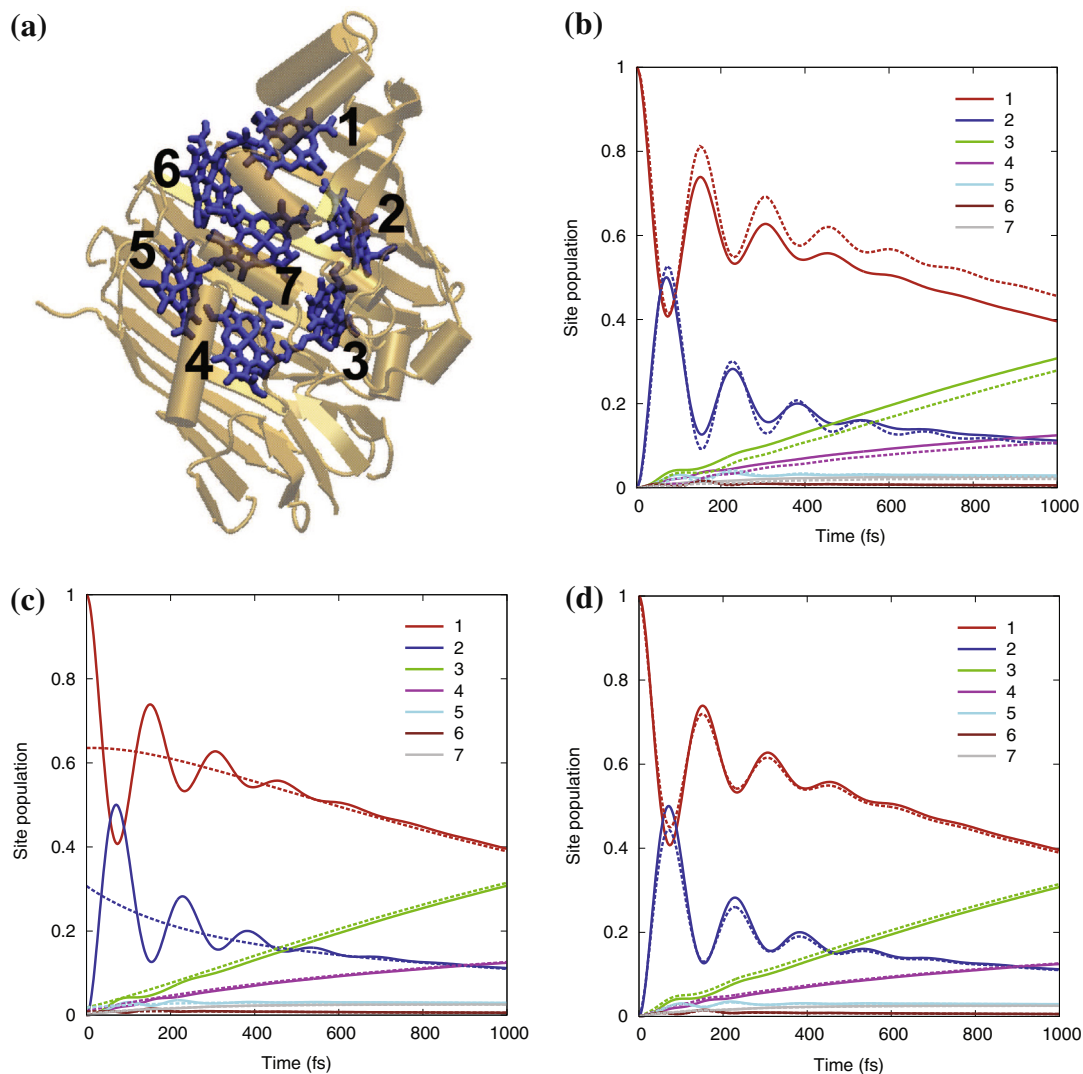


**Fig. 3.** Population dynamics of the FMO complex. (a) The pigment arrangements in the monomeric FMO complex (b) population dynamics simulated with CMRT (solid lines) compared to the numerically exact hierarchy equation of motion approach (dashed lines). (c) CMRT (solid lines) vs. original modified Redfield theory (dashed lines). The original modified Redfield equation can not handle site-localized initial conditions, therefore we select a different initial condition to reproduce the long-time dynamics. (d) non-Markovian CMRT (solid lines) vs. Markovian CMRT (dashed lines).

light harvesting [48]. In particular, in the past few years FMO has become the prototypical model for theoretical simulations of photosynthetic systems.

We simulate EET dynamics following site 1 of the FMO complex is excited using the parameters developed by Ishizaki and Fleming at 77 K [49]. In Fig. 3(b), we compared the CMRT method to the numerically exact reduced hierarchy equation of motion approach [49]. Clearly, the main features of the coherent dynamics simulated with CMRT coincide with the reduced hierarchy equation of motion results. In particular, the population transfer rates and dephasing rates are well reproduced, showing that CMRT provides excellent results for EET in photosynthetic systems. The only noticeable discrepancy is the difference in the long-time equilibrium populations. This discrepancy can be attributed to the exciton basis used in the CMRT approach, because the basis neglects exciton–phonon coupling effects in the equilibrium states. Moreover, note that in the reduced hierarchy equation of motion calculated performed by Ishizaki et al., a high-temperature approximation in the long time dynamics is used, which is also likely to contribute to the slippage shown in Fig. 3(b). Given that CMRT requires much less computational resources, we expect the CMRT approach to be a useful method for the investigation of EET dynamics in large photosynthetic systems. We remark that we present the dynamics using the artificial initial condition in the site representation only to emphasize the coherence effects, and the oscillatory coherences in the site representation should not be directly compared to experimentally observed quantum beatings in the two-dimensional electronic spectra.

Compared with the original modified Redfield equation, the most important feature of CMRT is the inclusion of coherence dynamics. Shown as the dash-dotted lines in Fig. 3(c), the modified Redfield equation does not describe any coherent dynamics, leading to monotonically decay and rise dynamics for site populations. The omission of coherences also leads to a slippage at the initial population, because the site localized initial condition can not be described by the modified Redfield theory that considers exciton populations only. This limitation actually restricts the applications of modified Redfield theory in many important problems. Instead, CMRT (solid lines) successfully describes the oscillating feature of the coherent dynamics, starting right from the site 1 initial state.

Additionally, we investigate the influence of non-Markovian effects in Fig. 3(d). Markovian and Non-Markovian CMRT predict similar dynamics in the FMO complex, in agreement with physical intuition that in photosynthetic systems the bath correlation time scales are much shorter than the system dynamics. We conclude that while several approximations have been used to derive CMRT, the approach still provides excellent results for photosynthetic systems. Therefore we have successfully extend the modified Redfield theory to provide an accurate, efficient method for EET dynamics in photosynthetic systems.

## 5. Conclusions

In this work, we apply the cumulant expansion approach to extend the modified Redfield theory to treat coherent dynamics and to include correlated bath and non-Markovian effects. This coherent modified Redfield theory provides a general framework to treat coherent EET dynamics with general initial conditions and bath types for molecular systems, allowing reliable simulation of spectrum and EET dynamics for photosynthetic systems. Notably, the CMRT equation of motion (Eq. (19)) can be casted in a generalized Lindblad form [50], therefore the positivity is conserved and the non-Markovianity can be quantified [38,51].

We have demonstrated the applications of this new framework to simulate EET dynamics in a simple two-site system and the FMO complex. From the numerical calculations of EET dynamics in the

two-site system, we concluded that CMRT performs excellently in a broad parameter regime investigated here. The exception is that it gives over-estimated rate for systems with small site-energy gaps under strong exciton–phonon couplings. In that case a combined Redfield–Förster picture could remedy the problem [32,52,30]. We have also applied the CMRT approach to simulate the population dynamics in the FMO complex, and the results are in excellent agreement with those calculated from the reduced hierarchy equation of motion method. This comparison shows that the CMRT approach is useful for modeling dynamics in light-harvesting complexes. Moreover, this approach accurately treats coherent dynamics with various couplings while retaining high computational efficiency, which is an advantage over many numerically exact frameworks. Finally, we remark that this work aims to present the derivation of the CMRT and the usefulness of CMRT in describing coherent EET dynamics. A detailed study of the applicable parameter regimes of the CMRT is beyond the scope of this work and is a work in progress. The benchmark results will be published elsewhere.

Note that although our discussions so far have focused on EET, charge transfer processes can be described within essentially the same framework. Therefore, we expect the coherent modified Redfield theory to be a useful theory for coherent charge transfer processes. Thus we have successfully developed a simple yet powerful framework for electronic dynamics and spectroscopy for molecular systems.

## Conflict of interest

The authors declare that there are no conflict of interest.

## Acknowledgments

We thank Pan-Pan Zhang for the QUAPI data and Akihito Ishizaki for kindly providing the HEOM data for FMO. YCC thanks the Ministry of Science and Technology, Taiwan (Grant No. NSC 100-2113-M-002-008-MY3), National Taiwan University (Grant No. 103R891305), and Center for Quantum Science and Engineering (Subproject: 103R891401) for financial support. We are grateful to Computer and Information Networking Center, National Taiwan University for the support of high-performance computing facilities. We are grateful to the National Center for High-performance Computing for computer time and facilities.

## References

- [1] R.J. Cogdell, A.T. Gardiner, H. Hashimoto, T.H.P. Brotsudarmo, *Photochem. Photobiol. Sci.* 7 (2008) 1150.
- [2] G.D. Scholes, G.R. Fleming, A. Olaya-Castro, R. van Grondelle, *Nature* 3 (2011) 763.
- [3] L.A. Pachon, P. Brumer, *Phys. Chem. Chem. Phys.* 14 (2012) 10094.
- [4] V. Novoderezhkin, R. van Grondelle, *J. Phys. Chem. B* 117 (2013) 11076.
- [5] G.S. Engel, T.R. Calhoun, E.L. Read, T.-K. Ahn, T. Mancal, Y.-C. Cheng, R.E. Blankenship, G.R. Fleming, *Nature* 446 (2007) 782.
- [6] E. Collini, G.D. Scholes, *Science* 323 (2009) 369.
- [7] E. Collini, C.Y. Wong, K.E. Wilk, P.M.G. Curmi, P. Brumer, G.D. Scholes, *Nature* 463 (2010) 644.
- [8] G. Panitchayangkoon, D. Hayes, K.A. Fransted, J.R. Caram, E. Harel, J. Wen, R.E. Blankenship, G.S. Engel, *Proc. Natl. Acad. Sci.* 107 (2010) 12766.
- [9] S. Jang, Y.-C. Cheng, D.R. Reichman, J.D. Eaves, *J. Chem. Phys.* 129 (2008) 101104.
- [10] A. Kolli, A. Nazir, A. Olaya-Castro, *J. Chem. Phys.* 135 (2011) 154112.
- [11] D.P.S. McCutcheon, A. Nazir, *J. Chem. Phys.* 135 (2011) 114501.
- [12] L. Yang, M. Devi, S. Jang, *J. Chem. Phys.* 137 (2012) 024101.
- [13] H. Zhu, V. May, B. Roeder, *Chem. Phys.* 351 (2008) 117.
- [14] G. Tao, W.H. Miller, *J. Phys. Chem. Lett.* 1 (2010) 891.
- [15] T.C. Berkelbach, T.E. Markland, D.R. Reichman, *J. Chem. Phys.* 136 (2012) 084104.
- [16] Tanimura, *Phys. Rev. A* 41 (1990) 6676.
- [17] R.-X. Xu, Y. Yan, *Phys. Rev. E* 75 (2007) 031107.
- [18] A. Ishizaki, Y. Tanimura, *Chem. Phys.* 347 (2008) 185.
- [19] A. Ishizaki, G.R. Fleming, *J. Chem. Phys.* 130 (2009) 234111.

- [20] N. Renaud, M.A. Ratner, V. Mujica, *J. Chem. Phys.* 135 (2011) 075102.
- [21] P. Nalbach, A. Ishizaki, G.R. Fleming, M. Thorwart, *New J. Phys.* 13 (2011) 063040.
- [22] Y.J. Yan, *Chem. Phys.* (2014) 140.
- [23] J.M. Moix, Y. Zhao, J. Cao, *Phys. Rev. B* 85 (2012) 115412.
- [24] J.M. Moix, J. Cao, *J. Chem. Phys.* 139 (2013) 134106.
- [25] X. Chen, J. Cao, R.J. Silbey, *J. Chem. Phys.* 138 (2013) 224104.
- [26] W. Zhang, T. Meier, V. Chernyak, S.J. Mukamel, *Chem. Phys.* 108 (1998) 7763.
- [27] M. Yang, G. Fleming, *Chem. Phys.* 282 (2002) 161.
- [28] V.I. Novoderezhkin, R. van Grondelle, *Phys. Chem. Chem. Phys.* 12 (2010) 7352.
- [29] V.I. Novoderezhkin, A.B. Doust, C. Curutchet, G.D. Scholes, R. van Grondelle, *Biophys. J.* 99 (2010) 344.
- [30] T. Renger, M.E.-A. Madjet, M. Schmidt Am Busch, J. Adolphs, F. Müh, *Photosynth. Res.* 116 (2013) 367.
- [31] V. Novoderezhkin, M. Palacios, H. van Amerongen, R. van Grondelle, *J. Phys. Chem. B* 108 (2004) 10363.
- [32] V. Novoderezhkin, A. Marin, R. van Grondelle, *Phys. Chem. Chem. Phys.* 13 (2011) 17093.
- [33] S. Jang, Y. Jung, R.J. Silbey, *Chem. Phys.* 275 (2002) 319.
- [34] A. Golosov, D. Reichman, *J. Chem. Phys.* 115 (2001) 9848.
- [35] A.A. Golosov, D.R. Reichman, *J. Chem. Phys.* 115 (2001) 9862.
- [36] S. Mukamel, *Principles of Nonlinear Optical Spectroscopy*, Oxford University Press, Oxford, 1995.
- [37] H.-P. Breuer, F. Petruccione, *The Theory of Open Quantum Systems*, Oxford University Press, Oxford, 2002.
- [38] H.-P. Breuer, *Phys. Rev. A* 75 (2007) 022103.
- [39] A. Ishizaki, G.R. Fleming, *J. Chem. Phys.* 130 (2009) 234110.
- [40] J. Olsina, T. Mancal, *J. Mol. Model.* 16 (2010) 1765.
- [41] P. Kumar, S. Jang, *J. Chem. Phys.* 138 (2013) 135101.
- [42] G. Panitchayangkoon, D.V. Voronine, D. Abramavicius, J.R. Caram, N.H.C. Lewis, S. Mukamel, G.S. Engel, *Proc. Natl. Acad. Sci.* 108 (2011) 20908.
- [43] H.-T. Chang, P.-P. Zhang, Y.-C. Cheng, *J. Chem. Phys.* 139 (2013) 224112.
- [44] T.-C. Yen, Y.-C. Cheng, *Proc. Chem.* 3 (2011) 211.
- [45] A. Gelzinis, D. Abramavicius, L. Valkunas, *Phys. Rev. B* 84 (2011) 245430.
- [46] C.K. Lee, J. Moix, J. Cao, *J. Chem. Phys.* 136 (2012) 204120.
- [47] M.S.A. Busch, F. Müh, M.E.-A. Madjet, T. Renger, *J. Phys. Chem. Lett.* 2 (2011) 93.
- [48] J.M. Olson, *Photosynth. Res.* 80 (2004) 181.
- [49] A. Ishizaki, G.R. Fleming, *Proc. Natl. Acad. Sci.* 106 (2009) 17255.
- [50] Q. Ai, Y.-J. Fan, B.-Y. Jin, Y.-C. Cheng, *New J. Phys.* 16 (2014) 1.
- [51] E.-M. Laine, J. Piilo, H.-P. Breuer, *Phys. Rev. A* 81 (2010) 062115.
- [52] D.I.G. Bennett, K. Amarnath, G.R. Fleming, *J. Am. Chem. Soc.* 135 (2013) 9164.